




REGULAR ARTICLE

Improving the Performance of CZTS/CZTSSe Tandem Thin Film Solar Cell

Loumafak Hafai^{1,2}, Mostefa Maache^{1,3,*} , Mohamed Wahid Bouabdelli⁴

¹ Department of Physics, FECS, Ziane Achour University, 17000 Djelfa, Algeria

² Physico Chemistry of Materials and Environment Laboratory, Ziane Achour University of Djelfa, BP 3117, Djelfa, Algeria

³ PLTFA, Physical Laboratory of Thin Films and Applications, Mohamed Khider University, 07000 Biskra, Algeria

⁴ Laboratory for analysis and Control of Energy Systems and Electrical Networks, Faculty of Technology, Amar Telidji University, BP 37G, 03000 Laghouat, Algeria

(Received 10 December 2023; revised manuscript received 14 April 2024; published online 29 April 2024)

Numerical simulation of CZTS/CZTSSe tandem solar cells utilizing Silvaco-Atlas was investigated. Firstly, the performances of conventional CZTS/CdS/ZnO and CZTSSe/CdS/ZnO single solar cells with thicknesses for both absorber layers at 360 nm and 3 nm, respectively, were studied independently. A wide band gap CZTS thin-film cell and a narrow band gap CZTSSe-based cell present conversion efficiencies of 11.10% and 13.76% respectively. This agrees with experimental and simulation results previously published. Furthermore, a CZTS/CZTSSe tandem cell configuration is identified keeping the identical material properties. A good conversion efficiency of 25.27% was obtained. Finally, the thickness of the CZTS adsorption layer of the top cell was optimized as a crucial factor to enhance the tandem performance. Optimal thickness coinciding to a highest efficiency of 26.05% is 420 nm. The output parameters obtained are, $J_{sc} = 28.46 \text{ mA/cm}^2$, $V_{oc} = 1.27 \text{ V}$ and $FF = 71.83\%$. This suggested results may help in the future research and may lead to the fabrication of CZTSSe-based solar cells.

Keywords: CZTS, CZTSSe, Solar cell, Tandem, Efficiency, Silvaco-Atlas.

DOI: [10.21272/jnep.16\(2\).02018](https://doi.org/10.21272/jnep.16(2).02018)

PACS numbers: 78.20.Bh, 73.40.Lq, 84.60.Jt

1. INTRODUCTION

Although there are several problems in the world, the energy crisis is what the scientific and intellectual community cares about the most, especially renewable energy, most importantly solar energy and how to exploit it. The sun has great potential to reply and satisfy the global demand for electricity, its rays can be converted using solar cells into electricity. Among the obstacles facing the exploits of solar energy is the lack of photovoltaic materials with a high conversion efficiency in solar cells [1]. The CdTe and CIGS thin-film solar cells possess good photo-conversion efficiency, though they use rare earth metals as raw materials for the absorbent layers, like Indium and Gallium, as well as cadmium and tellurium which are toxic materials [2,3]. Kesterite $\text{Cu}_2\text{ZnSn}(\text{S,Se})_4$ (CZTSSe) quaternary semiconductor is a favored material for photovoltaic cells that will replace the above materials, and due to its good photovoltaic properties, high absorption coefficient, and direct band gap [4–7]. The bandgap energy of the CZTSSe layers varies betwixt 1 and 1.5 eV, depending on the Sulfur/Selenium ratio [6,8–10]. The CZTSSe based solar cells have a middle efficiency in comparison to commercial cells based on CIGS, where it is approximately 11% for CZTS cells and it is about 13% for CZTSSe [11]. A dual-junction solar cell consisting of two sub-cells stacked together will have a higher conversion efficiency because it absorbs a wide range of

solar spectrum wavelengths. In this sense, we use tandem solar cells, which are devices with two or more absorbing layers of different optical band gaps.

Tandem solar cells are able to use incident sunlight more effectively and greater than single junction solar cells. To model and simulate the CZTS/CZTSSe tandem solar cell, and to optimize its performance, this study has been done. Tandem solar cells can capture the maximum number of photons, where the top cell of the tandem configuration employs high-band gap materials to absorb high-energy photons, whereas the bottom sub-cell uses low band gap materials to absorb low-energy photons transmitted via the top cell [12]. Accordingly, CZTS and costs based solar cells were placed at the top and bottom cells, respectively, in the proposed tandem design. Recently, a series of CZTS/CZTSSe based tandem solar cells about different configurations have proven highly effective with different conversion efficiencies (η). Where the CZTS ($E_g = 1.5 \text{ eV}$) was utilized as the absorber layer in the top cell and the CZTSSe ($E_g = 1.1 \text{ eV}$) in the bottom cell, the obtained efficiency $\eta = 15\%$. In aim to reduce the recombination losses and enhance the optical behavior, A.E. Benzetta et al. added in the back of CZTS top cell layer of back surface field (BSF) and they obtained $\eta = 19.25\%$ [13]. U. Saha et al., and after optimizing the band gap they got $\eta = 21.74\%$ [14].

Simulation studies on CZTS/CZTSSe tandem thin film solar cells are reported insufficiently. In this

* Correspondence e-mail: m.maache@univ-djelfa.dz



study, single and tandem CZTS/CZTSSe based solar cells were investigated using the Silvaco-Atlas simulator. To start, a comparative study based on the simulation results of CZTS and CZTSSe single solar cells versus those formerly published was carried out. Next, the numerical study will demonstrate how CZTS/CZTSSe tandem thin film solar cells help to achieve ultra-high efficiency. Tandem thin film solar cell configurations appear to have a promising future. Such a study will help the experimental scientist to optimize this cell which exceeds the performance of optimized single solar cell.

2. STRUCTURAL AND NUMERICALSIMULATION

In order to get higher efficiencies, CZTS/CZTSSe tandem thin film solar cell comprised seven layers was constructed by stacking together two single solar cells. Starting with the top cell, the layers are as follows: ZnO/n-CdS/p-CZTS/ZnO/n-CdS/p-CZTSSe/Mo, where Molybdenum (Mo) is a back contact (Ohmic contact) and the top ZnO is used as a transparent conducting oxide layer (TCO). Fig. 1 shows the schematic of investigating tandem thin film solar cell configuration, according to the design reported by other research, such as CIGS/CIGS tandem solar cells [15,16].

Therefore, the final tandem cell consists of two single cells, CZTS as the top cell and CZTSSe as the bottom one. Wide band gap absorber layer CZTS ($E_g = 1.5$ eV) has a teeny thickness, and weak band gap ($E_g = 1.13$ eV) CZTSSe thicker absorber layer, which correspond to the optimal experimental values [6,17]. The structure was studied under the solar spectrum AM1.5, with an incident power density of 100 mW/cm² at room temperature $T = 300$ K.

Table 1 shows different values of the physical parameters of the all materials were used as inputs in Silvaco-Atlas software. These photovoltaic parameters were adopted from the literature [17–24].

Silvaco–Atlas physically- based on main basic semiconductor equations to simulate semiconductor devices, such as Poisson's equation and the continuity equation for holes and electrons [15,23,25].

The current-voltage (I-V) equation of a solar cell is the superposition of the photo-current I_{ph} and the dark current. It is expressed following the famous Shockley equation as follows:

$$I = I_{ph} - I_0 \left(\exp\left(\frac{qV}{akT}\right) - 1 \right) \quad (1)$$

where I_{ph} is the photo-current, I_0 is the reverse saturation current, q is the absolute value of electron charge,

a is the ideality factor, k is Boltzmann's constant and T is absolute temperature.

The main solar cell parameters characterize its performance are ordered as follows [26,27]:

- The short-circuit current (I_{sc})

$$I_{sc} = I_{ph} \quad (2)$$

Is the current that flows through the solar cell, when there is no voltage across it: $I_{sc} = I(V = 0)$. In the ideal case, I_{sc} is equal to the photo-current I_{ph} .

- The open-circuit voltage V_{oc}

It is the highest voltage available from a solar cell, and this occurs when there is no current.

V_{oc} can be calculated based on equation (3):

$$V_{oc} = \frac{akT}{q} \ln\left(\frac{I_{ph}}{I_0}\right) \quad (3)$$

- The fill factor FF

It is defined as follows:

$$FF = \frac{P_{max}}{V_{oc} I_{sc}} \quad (4)$$

P_{max} is the maximum power

- The conversion efficiency (η)

It is the most significant parameter in solar cell design. Equation (5) represents the efficiency relationship in relation to other parameters:

$$\eta = \frac{P_{max}}{P_{in}} = \frac{V_{oc} I_{sc} FF}{P_{in}} \quad (5)$$

P_{in} is the incident optical power.

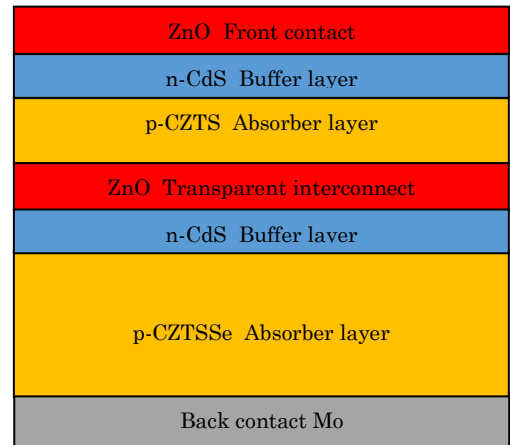


Fig. 1 – Tandem solar cell CZTS/CZTSSe design

Table 1 – Material parameters for CZTS/CZTSSe tandem solar cell used in simulation

Parameters	p-CZTS	p-CZTSSe	n-CdS	n-ZnO
Electron affinity (eV)	4.5	4.2	4.2	4.5
Band gap (eV)	1.5	1.13	2.4	3.3
Permittivity (F cm ⁻¹)	10	13.6	10	9
CB effective density of states (cm ⁻³)	2.2×10 ¹⁸	2.2×10 ¹⁸	2.2×10 ¹⁸	2.2×10 ¹⁸

VB effective density of states (cm^{-3})	1.8×10^{19}	1.8×10^{19}	1.8×10^{19}	1.8×10^{19}
Electron mobility ($\text{cm}^2/\text{V s}$)	100	100	100	100
Hole mobility ($\text{cm}^2/\text{V s}$)	25	25	25	25
Defect density (cm^{-3})	10^{14}	10^{14}	10^{17}	/

3. RESULTS AND DISCUSSION

Firstly, CZTS and CZTSSe individual junction solar cells were simulated independently adopting the several simulation parameters mentioned in Table 1. Conversion efficiency (η), short circuit current (J_{sc}), open circuit voltage (V_{oc}), and fill factor (FF) are the primary factors affecting solar cell achievement and its performance. So in this work we'll focus on these parameters.

3.1 Modeling of a CZTS single top cell

Conventional thin film solar cell CZTS is designed by placing an absorber layer of CZTS on Mo-coated glass substrate Fig. 2(a), above it a buffer CdS layer, followed by a ZnO transparent conductive oxide layer. As we mentioned above, CZTS thin film solar cell with thicknesses correspond to suitable bandgap energy ($E_g = 1.5 \text{ eV}$). This design was optimized to enhance the conversion efficiency. The obtained current-voltage curve of basic CZTS solar cell is presented in Fig. 2 (b).

Table 2 summarizes the results of our simulations alongside other published simulated and experimental data. By comparison, it can be observed that our results agree with the other simulation results [28] and the experimental data [11], which validate our model simulation and selected material's parameters.

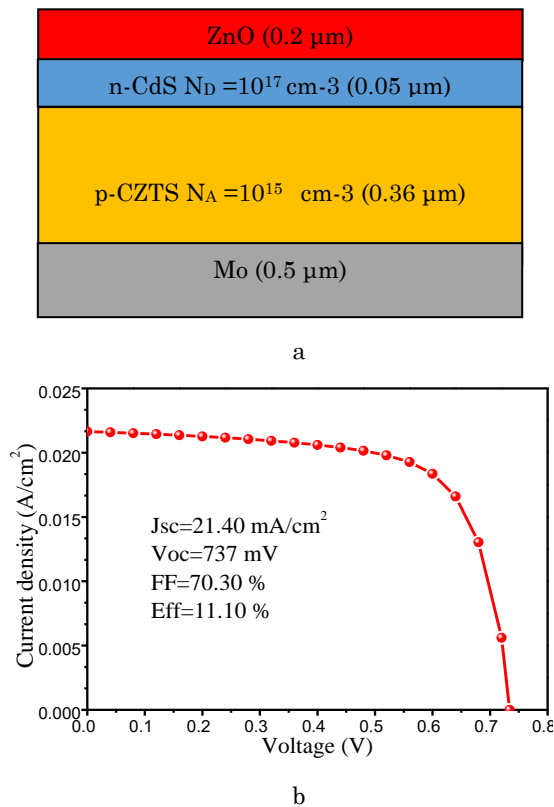


Fig. 2 – Basic CZTS single solar cell (a) structure, (b) Current-voltage curve

Table 1 – Characteristics of the simulated CZTS single top solar cell, as well as other experimental and simulated parameters.

Performance parameters	This work	Experiment [11]	Simulated [28]
J_{sc} (mA/cm^2)	21.40	21.74	22.31
V_{oc} (mV)	737	730	715
FF (%)	70.30	69.3	69.25
Efficiency η (%)	11.10	11	11.05

3.2 Modeling of a CZTSSe bottom cell

The standard CZTSSe thin film single bottom solar cell structure is formed by an absorber layer of CZTSSe (p-type) deposited on Mo-coated glass substrate (back contact), above it a buffer layer of CdS (n -type) with layer thicknesses corresponding to bandgap energy of 1.13 eV, followed by a ZnO transparent conductive oxide layer (contact) is the top of the structure, as is shown in Fig. 3(a). Current-voltage characteristics are given in Fig. 3(b).

We compare our simulation results with those of other simulation and experimental results given in Table 3. Whence, it is clear that all performance parameters of our simulated cell show a higher value than those in the simulated one [19] and very close to those of the experimental cell [29]. Also, these obtained results validate our model simulation and approve the chosen parameters.

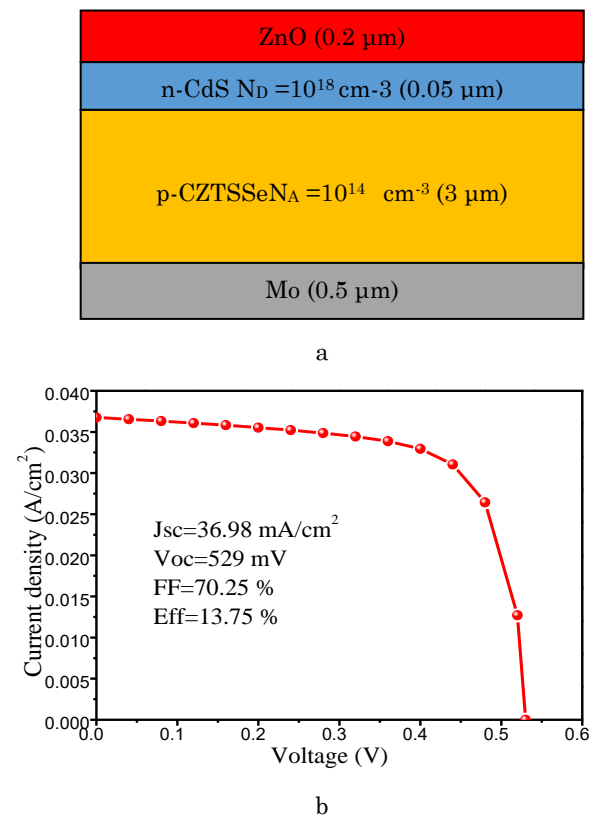


Fig. 3 – Basic CZTSSe single solar cell (a) structure, (b) Current-voltage curve

Table 3 – Performance parameters of the simulated CZTSSe single bottom solar cell, as well as other experimental and simulated parameters.

Performance parameters	This work	Experiment [29]	Simulated [19]
J_{sc} (mA/cm ²)	36.98	36.18	35.32
V_{oc} (mV)	529	537	536
FF (%)	70.25	69.8	68.94
Efficiency η (%)	13.75	13.6	13.13

The obtained simulation results show that the CZTS single top solar cell has a high V_{oc} (737 mV) and a low J_{sc} (21.40 mA/cm²) mainly due to its large band gap. On the other hand, and oppositely to the top cell, the bottom single solar cell CZTSSe has lower V_{oc} of 529 mV and higher J_{sc} of 36.98 mA/cm² because of its lower band gap energy, which allows absorption of low energy photons (longer wavelength) and leads to increase the photocurrent [30]. Which supports our choice of this type of solar cells compared to those of the CIGS thin film solar cells as reported in [31], to achieve high efficiency.

Fig. 4 presents the External Quantum Efficiency (EQE) spectrum of the CZTS, CZTSSe solar cells between 300 and 1110 nm. Both CZTS and CZTSSe EQE spectrum response presents maximum value at 55 μm indicating a high recombination rate. Significant decrease in CZTS spectrum for wavelengths beyond 0.55 μm , which signifies very elevated recombination losses in the CZTS layer near the Mo layer, hence a lower J_{sc} [32].

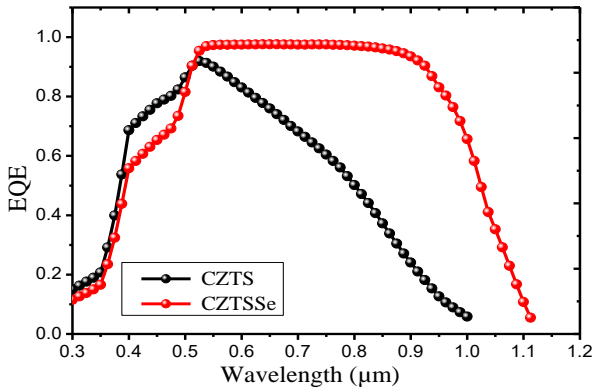


Fig. 4 – External Quantum Efficiency for CZTS and CZTSSe single solar cells versus wavelength.

The reduction of EQE spectrum in higher energy photons (short wavelengths) part is attributed to the absorption losses in the buffer and window layers (CdS and ZnO) or to surface recombination at the top.

However, the EQE spectrum of CZTSSe shows high value in large area of the visible range, owing to the smaller band gap of CZTSSe, which allows photons to participate in photocurrent generation, and consequently in the increase of CZTSSe single solar cell J_{sc} [33].

Via these obtained results of CZTSSe and CZTS solar cells, it is estimated that we can use them as a tandem solar cell design, CZTS in a top cell and CZTSSe as a bottom cell due to the promising value of quantum efficiency in the range visible ($\geq 90\%$).

3.3 Modeling of a CZTS/CZTSSe tandem cell

CZTSS/CZTSSe tandem thin film solar cell configuration is presented in Fig. 5. In the top cell, the cathode and the anode were positioned at the front contact ZnO and the transparent interconnect ZnO layer, respectively. While, in the bottom cell, the cathode and the anode contacts were placed at the interconnect ZnO and the back Mo layer, respectively.

Fig. 6 shows the variation curves of the current density J with the applied voltage V of the bottom, top, and tandem cells. They are arranged together, and the Pv parameters extracted from these curves are specified in Table 4.

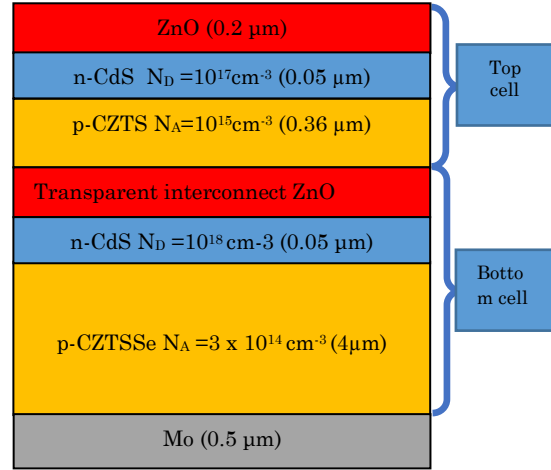


Fig. 5 – CZTS/CZTSSe tandem solar cell structure

The conversion efficiencies of the CZTS and CZTSSe top and bottom solar cells are 13.88% and 10.48% respectively. CZTS/CZTSSe tandem cell achieve a conversion efficiency of 25.27%. The enhancement of the CZTS/CZTSSe tandem cell configuration appears in term of a better open circuit voltage (1.26 V) which is equal to the summation of their top and bottom single cells voltages (0.737 V and 0.529 V), and J_{sc} (27.33 mA/cm²) which is limited by the lowest current from CZTS top cell ($J_{sc} = 27.02$ mA/cm²) [19]. These values are consistent with the series-connected circuit principles. So, the CZTS/CZTSSe tandem thin film solar cell operates effectively. An improvement in the efficiency of the CZTS top cell is observed, because it receives the whole solar spectrum compared to CZTSSe bottom cell in CZTS/CZTSSe tandem, however the bottom cell is exposed to less sunlight, it receives only the remaining solar spectrum transmitted by the top cell. The conversion efficiency of the tandem cell is better than those of the CZTS and CZTSSe single cells (11.10% and 13.75%). By comparison with preceding simulation works which used SCAPS-1D simulator, CZTS/CZTSSe tandem cells achieve optimum conversion efficiencies of 19.25% [19], using Silvaco-Atlas software, the obtained conversion efficiency of 25.27% for the non-optimized tandem thin film solar cell is close to that obtained by A.E. Benzetta et al. (2021), and by M.A. Green et al (2022) [19,29].

For an ideal tandem cell, the current matched condition should be achieved ($J_{sc}(Tandem) = J_{sc}(Top) = J_{sc}(Bottom)$) [8]. So, the CZTSSe

bottom cell absorber thickness was set at 3 μm and the CZTS top cell absorber thickness was varied from 0.2 μm to 0.6 μm to achieve the optimal current of the ideal tandem solar cell. The $J_{sc}(\text{Top})$ and $J_{sc}(\text{Bottom})$ versus the thickness of CZTS absorber layer are presented in Fig. 7. The intersection of the curves reveals a value of $J_{sc} = 28.46 \text{ mA/cm}^2$ for both cell matches for a top cell absorber thickness of about 0.42 μm .

Fig. 8 shows the resulted J-V characteristics of the CZTS top cell, CZTSSE bottom cell, and for the optimal structure of the CZTS/ CZTSSE tandem cell. The optimized thickness of CZTS top cell absorber yield to 14.90%, 10.61% and 26.05% efficiencies of top, bot-tom and tandem cells, respectively, with $V_{oc}=1.27 \text{ V}$, corresponding to the sum of the single voltages of the CZTS and CZTSSE cells (0.75 V and 0.52 V respectively) and the $J_{sc(\text{tandem})} = 28.46 \text{ mA/cm}^2$, as can be seen in Table 4. These results are better than the previous values before optimization.

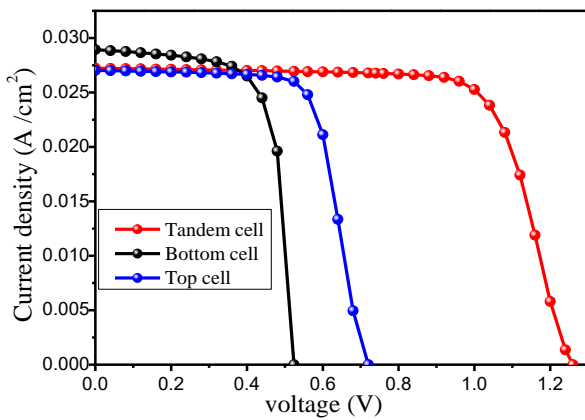


Fig. 6– The J-V for the CZTS top cell, CZTSSE bottom cell, and the CZTS/CZTSSE tandem cell.

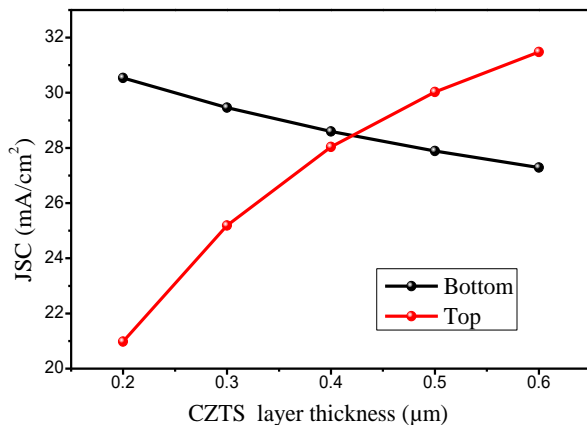


Fig. 7 – The J_{sc} versus the thickness of CZTS absorber layer for both top and bottom cells.

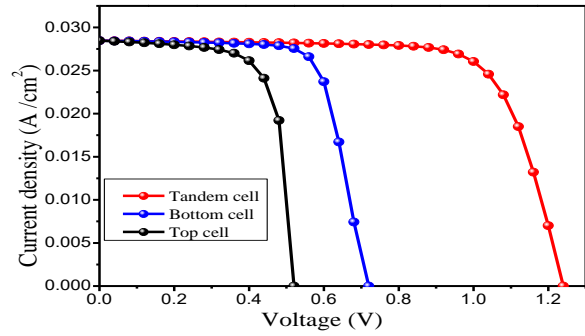


Fig. 8– The J-V for the CZTS top cell, CZTSSE bottom cell and CZTS/CZTSSE tandem cell after optimization.

Table 4– Electrical parameters of CZTS top cell, CZTSSE bottom cell and optimized CZTS/ CZTSSE tandem cell.

Performance parameters	Our simulated tandem cell after optimization		
	Top cell	Bottom cell	Tandem cell
$J_{sc} \text{ (mA/cm}^2\text{)}$	28.46	28.46	28.46
$V_{oc} \text{ (mV)}$	0.75	0.52	1.27
$FF \text{ (%)}$	49.81	71.13	71.83
Efficiency $\eta \text{ (%)}$	14.90	10.61	26.05

4. CONCLUSION

In this study, numerical simulation of a new CZTS/CZTSSE tandem thin film solar cell structure was investigated using Silvaco-Atlas software under AM1.5. Firstly, the top cell CZTS and the bottom cell CZTSSE were simulated individually. The optimized top and bottom sub-cell was determined, with the conversion efficiency of 11.10% and 13.76% respectively. Secondly, the tandem CZTS/CZTSSE solar thin film cell consists of optimize sub-cells was simulated, an enhancement in the conversion efficiency to 25.27% was obtained. Thickness of the CZTS absorber layer of the top cell was considered as a key parameter to ameliorate the performance of the CZTS/CZTSSE tandem cell. Further, the top cell is evaluated at different thicknesses for tandem structure to find current matching condition. The optimum absorber layer's thickness of the CZTS top cell was 0.42 μm as a result. By matching the J_{sc} values between the sub-cells ($J_{sc}(\text{Tandem}) = J_{sc}(\text{Top}) = J_{sc}(\text{Bottom})$), the maximum power conversion efficiency 26.05% was achieved. This present work proves that a CZTS/CZTSSE tandem design enhances the solar cell performance due to the absorption of supplementary solar photons. Experimental realization of such tandem devices could be quite possible a cost-effective way to improve efficiency.

REFERENCES

- G. Wang, Z. Guo, C. Chen, W. Yu, B. Xu, B. Lin, *Sol. Energy* **236**, 576 (2022).
- K.-P. Kim, W.-L. Jeong, J.-S. Kim, J.-S. Lee, S.-H. Mun, H.-M. Kwak, D.-S. Lee, *J. Alloys Compd.* **910**, 164899 (2022).
- A.M. Curtin, C.A. Vail, H.L. Buckley, *Water-Energy Nexus*, **3**, 15 (2020).
- L. Sravani, S. Routray, M. Courel, K.P. Pradhan, *Sol. Energy* **227**, 56 (2021).
- C. Rachidy, B. Hartiti, S. Touhtouh, S. Moujoud, A. Faddouli, F. Belhora, M. Ertugrul, S. Fadili, M. Stitou, P. Thevenin, A. Hajjaji, *Mater. Today Proc.* **36**, 26 (2022).
- D. Zhang, S. Sun, X. Li, X. Li, X. Liu, Q. Li, H. Liao,

- S. Wang, *Sol. Energy* **227**, 516 (2021).
7. Y.H. Khattak, F. Baig, B.M. Soucase, S. Beg, S.R. Gillani, S. Ahmed, *Optik (Stuttg)* **171**, 453 (2018).
 8. A. Kumar, *Opt. Quant Electron* **53**, 528 (2021).
 9. P. Punathil, E. Artegianni, S. Zanetti, L. Lozzi, V. Kumar, A. Romeo, *Sol. Energy* **236**, 599 (2022).
 10. B. Eghbalifar, H. Izadneshan, G. Solookinejad, L. Separdar, *Solid State Commun.* **343**, 114654 (2022).
 11. M.A. Green, E.D. Dunlop, J. Hohl-Ebinger, M. Yoshita, N. Kopidakis, X. Hao, *Prog. Photovolt. Res. Appl.* **30**, 3 (2022).
 12. E. Raza, Z. Ahmad, *Energy Rep.* **8**, 5820 (2022).
 13. A.E. Benzetta, M. Abderrezek, M.E. Djeghlal, *Optik (Stuttg)* **242**, 167320 (2021).
 14. U. Saha, M.K. Alam, *RSC Adv.* **7**, 4806 (2017).
 15. B. Bouanani, A. Joti, F.S. Bachir Bouiadjra, A. Kadid, *Optik (Stuttg)* **204**, 164217 (2020).
 16. M. Elbar, S. Tobbeche, *Energy Procedia* **74**, 1220 (2015).
 17. A. Hajjiah, *Micro Nanostruct.* **165**, 207204 (2022).
 18. H. Ferhati, F. Djeflal, B.L. Drissi, *Superlattice. Microstruct.* **148**, 106727 (2020).
 19. A.E. Benzetta, M. Abderrezek, M.E. Djeghlal, *Optik (Stuttg)* **242**, 167320 (2021).
 20. O.K. Simya, A. Mahaboobbatcha, K. Balachander, *Superlattice. Microstruct* **92**, 285 (2016).
 21. S.R. Meher, L. Balakrishnan, Z.C. Alex, *Superlattice. Microstruct.* **100**, 703 (2016).
 22. S. Padhy, R. Mannu, U.P. Singh, *Sol. Energy* **216**, 601 (2021).
 23. T. Joseph Mebelson, K. Elampari, *Today Proc.* **46**, 2540 (2021).
 24. A. Cherouana, R. Labbani, *Appl. Surf. Sci.* **424**, 251 (2017).
 25. A. Khadir, *Opt. Mater. (Amst)* **127**, 112281 (2022).
 26. B. Farhadi, M. Naseri, *Optik (Stuttg)* **127**, 10232 (2016).
 27. M.W. Bouabdelli, F. Rogti, M. Maache, A. Rabehi, *Optik (Stuttg)* **216**, 164948 (2020).
 28. S.E. Maklavani, S. Mohammadnejad, *Sol. Energy* **204**, 489 (2020).
 29. M.A. Green, E.D. Dunlop, J. Hohl Ebinger, M. Yoshita, N. Kopidakis, K. Bothe, D. Hinken, M. Rauer, X. Hao, *Prog. Photovolt. Res. Appl.* **30**, 687 (2022).
 30. T. Todorov, T. Gershon, O. Gunawan, C. Sturdevant, S. Guha, *Appl. Phys. Lett.* **105**, 173902 (2014).
 31. F. Ghamsari-Yazdel, A. Fattah, *Micro Nanostruct* **168**, 207289 (2022).
 32. J. Ge, J. Jiang, P. Yang, C. Peng, Z. Huang, S. Zuo, L. Yang, J. Chu, *Sol. Energy Mater. Sol. C* **125**, 20 (2014).
 33. G.K. Gupta, A. Dixit, *arXiv preprint arXiv:1801.08498* (2018).

Покращення продуктивності тандемної тонкоплівкової сонячної батареї CZTS/CZTSSe

Loumafak Hafifa^{1,2}, Mostefa Maache^{1,3}, Mohamed Wahid Bouabdelli⁴

¹ Department of Physics, FECS, Ziane Achour University, 17000 Djelfa, Algeria

² Physico Chemistry of Materials and Environment Laboratory, Ziane Achour University of Djelfa, BP 3117, Djelfa, Algeria

³ PLTFA, Physical Laboratory of Thin Films and Applications, Mohamed Khider University, 07000 Biskra, Algeria

⁴ Laboratory for analysis and Control of Energy Systems and Electrical Networks, Faculty of Technology, Amar Telidji University, BP 37G, 03000 Laghouat, Algeria

Методом чисельного моделювання з використанням Silvaco-Atlas досліджені параметри тандемних сонячних елементів CZTS/CZTSSe. По-перше, характеристики звичайних CZTS/CdS/ZnO та CZTSSe/CdS/ZnO окремих сонячних елементів із товщиною обох шарів поглинача 360 нм та 3 нм відповідно були досліджені незалежно. Тонкоплівкова комірка CZTS з широкою забороненою зоною та комірка на основі CZTSSe з вузькою забороненою зоною мають ефективність перетворення 11,10 % і 13,76 % відповідно. Це узгоджується з результатами експериментів і моделювання, опублікованими раніше. Крім того, ідентифікується конфігурація тандемної клітини CZTS/CZTSSe, яка зберігає ідентичні властивості матеріалу. Отримана висока ефективність перетворення 25,27 %. Товщина адсорбційного шару CZTS верхньої комірки була оптимізована як вирішальний фактор для підвищення продуктивності тандему. Оптимальна товщина, яка збігається з найвищою ефективністю 26,05%, становить 420 нм. Отримані вихідні параметри: $J_{sc} = 28,46 \text{ mA/cm}^2$, $V_{oc} = 1,27 \text{ V}$ і $FF = 71,83 \%$. Ці запропоновані результати можуть допомогти в майбутніх дослідженнях і призвести до виготовлення сонячних елементів на основі CZTSSe.

Ключові слова: CZTS, CZTSSe, Сонячна батарея, Ефективність, Silvaco-Atlas.